Langerhans Cells Facilitate UVB-induced Epidermal Carcinogenesis

Julia M. Lewis, **Christina D. Bürgler**, **Marianna Freudzon**, **Kseniya Golubets**, **Juliet F. Gibson**, **Renata B. Filler**, and **Michael Girardi**

Department of Dermatology, Yale School of Medicine, New Haven, Connecticut, U.S.A

Abstract

Ultraviolet B (UVB) light is considered the major environmental inducer of human keratinocyte DNA mutations, including within the tumor-suppressor gene p53, and chronic exposure is associated with cutaneous squamous cell carcinoma (SCC) formation. Langerhans cells (LC) comprise a dendritic network within the suprabasilar epidermis, yet the role of LC in UVB-induced carcinogenesis is largely unknown. Herein, we show that LC-intact epidermis develops UVB-induced tumors more readily than LC-deficient epidermis. While levels of epidermal cyclopyrimidine dimers (CPD) following acute UVB exposure are equivalent in the presence or absence of LC, chronic UVB-induced p53 mutant clonal islands expand more readily in association with LC which remain largely intact and are preferentially found in proximity to the expanding mutant keratinocyte populations. The observed LC facilitation of mutant p53 clonal expansion is completely αβ and γδ T-cell independent, and is associated with increased intraepidermal expression of interleukin (IL)-22 and the presence of group 3 innate lymphoid cells (ILC3). These data demonstrate that LC play a key role in UVB-induced cutaneous carcinogenesis, and suggest that LC locally stimulate keratinocyte proliferation and innate immune cells that provoke tumor outgrowth.

Keywords

interleukin-22; mutagenesis; carcinogenesis; squamous cell carcinoma; Langerhans cells; dendritic cells

INTRODUCTION

Chronic ultraviolet B (UVB) light exposure is a major risk factor for development of pre-malignant actinic keratoses (AK) and malignant SCC, each harboring frequent mutations in the master cell cycle regulator TP53 (p53) gene (Ziegler *et al.*, 1994). Initiating mutations

Address Correspondence: Michael Girardi, MD, Yale University School of Medicine, 333 Cedar Street, HRT 604D, New Haven, CT 06520-8059, United States, girardi@yale.edu, Tel: 203-785-4092, Fax: 203-785-7637.

Sites of experiments: New Haven, Connecticut, U.S.A.

largely result from unrepaired cyclopyrimidine dimers (CPD). Promoting oncogenetic alterations, e.g. RAS (Daya-Grosjean *et al.*, 1993) and NOTCH (Durinck *et al.*, 2011), may result from continued UV exposure, immune influences and other stimuli that drive keratinocyte (KC) proliferation, dedifferentiation, transformation, and ultimately tumor outgrowth (rev. in Epstein, 1983; Kripke, 1984). Situated adjacent to basal and folliculo-infundibullar KCs that give rise to AK and SCC neoplasia is a network of dendritic CD207+ (Langerin+) intraepidermal Langerhans cells (LCs) that 1) survey the epidermis (Nishibu *et al.*, 2006) for evidence of toxin/microbial penetration (Kubo *et al.*, 2009), and 2) serve as antigen-presenting cells (APC) for the activation T cells resident in the skin (Seneschal *et al.*, 2012) or after migration to draining lymph nodes (Kaplan *et al.*, 2005; Bobr *et al.*, 2012).

We have previously suggested that LC may function as key players in the epithelial-stress response, where they coordinate with resident γδ T cells and αβ natural killer T (NKT) cells (Strid *et al.*, 2008). γδ T cells (Girardi *et al.*, 2001, 2003), including resident γδ dendritic epidermal T cells (DETC) (Strid *et al.*, 2008, MacLeod *et al.*, 2014), may mediate diverse anti-tumor activities, while LC have been shown to facilitate chemical carcinogenesis by enhancing mutagenesis (Modi *et al.*, 2012) and tumor promotion (Lewis *et al.*, 2014). Moreover, the role of LC in the well-established phenomenon of UV-induced immune suppression is unclear, with some evidence suggesting that LC are not necessary (Wang *et al.*, 2009) and other studies suggesting that LC may play a critical role (Fukunaga *et al.*, 2010). Hence, we sought to determine whether locally resident LC influence events relevant to UV-induction of cutaneous SCC, and if so, whether such influences are dependent on adaptive and innate immunity afforded by αβ and/or γδ T cells. We utilized mice rendered genetically deficient in LC (Kaplan *et al.*, 2005), and/or αβ and γδ T cells, and studied the impact on several fundamental steps of UVB-induced cutaneous carcinogenesis including direct genotoxicity (CPD formation), p53 mutant clonal KC development and expansion, and tumor outgrowth. Herein, we reveal that LC exert T cell-independent pro-tumor effects largely via the promotion of clonal expansion in association with enhanced epidermal expression of interleukin (IL)-1β, IL-6, IL-23, and NOS2, as well as augmented expression of the epithelial growth factor IL-22. In addition we observe group 3 innate lymphoid cells (ILC3) capable of IL-22 production in chronically UVB irradiated epidermis. Furthermore, we identify a major T cell-independent role for LC in the regulation of the epidermal-stress response more generally.

RESULTS

LC enhance chronic UVB-induced cutaneous tumor outgrowth

To assess the collective effect of chronic UVB exposure on the emergence of cutaneous tumors, hairless (hr/hr) LC-deficient hu-Langerin-DTA (DTA) mice (Kaplan *et al.*, 2005) were compared to LC-intact normal littermate controls (NLC) for tumor induction by 3x weekly UVB irradiation of dorsal skin. LC-intact mice showed a substantially higher rate of UVB-induced tumor development (mean 5.10 ± 1.18 vs 2.44 ± 0.47 tumors/mouse at 18 weeks; $P=0.002$) (Figure 1a), as well as a greater accumulating tumor volume over this time (Figure 1b). UVB exposure has been shown to compromise intraepidermal LC numbers via

induction of apoptosis and stimulation of LC migration (Aberer *et al*., 1986; Nishibu *et al*., 2006). Thus, we considered the possibility that the observed pro-tumor influence of LC might be due to early events, e.g. specifically by facilitating KC DNA-damage.

LC do not affect UVB-induced CPDs in neighboring KC

In chemical carcinogenesis, LC are associated with DMBA-induced genotoxicity in adjacent KC (Modi *et al*., 2012). Since LC are also associated with accelerated UVB-induced tumor development, we considered the possibility that CPD formation might occur more readily in the presence of LC. Given that γδ DETC have shown the capacity to facilitate CPD repair (MacLeod *et al*., 2014) and LC and γδ DETC form tightly regulated cell contacts following epidermal stress (Strid *et al*. 2008), we also considered whether LC might effect the efficient repair of CPDs within KC. Groups of LC-intact (NLC) and LC-deficient (DTA) mice were irradiated with a single dose of 50 J/m^2 or 100 J/m^2 UVB, and epidermal sheets harvested at 1 hr to assess for acute UVB-induced CPD formation, and at 24 hr to assess CPD repair (Figure 2a, b; Supplementary Figure S1 online). CPDs were observed diffusely within basal KCs 1 hr after UVB exposure, significantly higher at 100 J/m^2 than 50 J/m^2 but indistinguishable between similarly exposed NLC and DTA mice. At 24 hr after UVB exposure, CPD level decreased comparably between NLC and DTA skin (Figure 2a, b), while LC numbers were maintained throughout (Figure 2c). These data suggest that LC do not significantly influence CPD formation following UVB-exposure, nor do they appear to affect DNA-repair in the first 24 hr following exposure. Thus, we focused further experiments on the effects of LC on keratinocytes during chronic UVB exposure.

LC numbers are largely maintained in chronically UVB-irradiated epidermis

Prior studies have demonstrated the sensitivity of LC to acute UVB-induced apoptosis, as well as the capacity of UVB to trigger LC migration to draining lymph nodes (Aberer *et al*., 1986; Nishibu *et al*., 2006). UVB can also precipitate epidermotropism and differentiation of peripheral blood Gr1+ monocytes into CD207+ DC (Merad *et al*., 2002) followed by a second wave of steady-state precursor-derived long-term LCs (Seré *et al*., 2012) to repopulate the LC compartment. Few studies, however, have quantified the net effects of chronic UVB exposure on the intrapepidermal LC population. Since it was unlikely that the increased tumor susceptibility observed in LC-intact skin (Figure 1) was due to LC enhancement of DNA-damage in adjacent KC (Figure 2), we hypothesized that under chronic low dose UVB exposure net LC numbers would remain largely intact. Untreated NLC and DTA mice displayed comparable γδ DETC density (Figure 3a–c), consistent with prior reports (Kaplan *et al*., 2005). Following 5 weeks chronic UVB exposure, within NLC mice we found the LC compartment was largely maintained; in contrast, intraepidermal γδ T cells were nearly eliminated in both NLC and DTA, consistent with the exquisite sensitivity (Ho *et al*., 1991) of DETC to UVB-induced apoptosis (Figure 3a–c).

LC promote p53 mutant KC clonal island expansion and are preferentially found in association with the p53 mutant islands

To address the potential role of LC in the enhancement of clonal expansion, hairless (hr/hr) LC-intact (NLC) and LC-deficient (DTA) mice were exposed to UVB, and p53 mutant KC

clonal islands quantified at 5 and 9 weeks (e.g. 6 to 10 weeks prior to tumor onset). "p53 islands" can be identified in UVB-exposed epidermis by staining with an antibody that binds to both native and mutant p53, but at markedly higher levels in KC harboring mutant p53 due to the absence of negative feedback. Direct sequencing of p53 has shown that such p53-immunopositive islands are mutant and clonal (Zhang *et al.*, 2001). To confirm active proliferation of the p53 mutant KC we performed co-staining with Ki-67 (Supplementary Figure S2 online). While p53 island number and basal area occupied were comparable between NLC and DTA mice at 5 weeks, NLC showed a >50% greater number of p53 islands and a >100% increase in the basal area involved at 9 weeks (Figure 3d, e; Supplementary Figure S3 online), with similar results seen when hair-bearing FVB.NLC and FVB.DTA mice were compared (Supplementary Figure S4 online).

Thus, persistent and/or repopulating LC are available in sufficient numbers under chronic UVB exposure to influence epidermal tumor outgrowth. Moreover, LC were preferentially found within or adjacent to p53 clonal islands (Figure 3f–i, Supplementary Figure S3 online), with a ~40% increase in LC density in association with the mutant KC after 9 weeks of chronic UVB exposure (Figure 3i, $617 \pm 35/mm^2$ island associated, $448 \pm 44/mm^2$ not associated, P=0.0065). Phenotypic analysis of LC isolated from chronic UVB-exposed epidermis revealed upregulation of CD207 and MHC-II, consistent with activation, but without changes in CCR7 or CXCR4 expression which might indicate an increased capacity for migration to draining LN (Supplementary Figure S5 online).

LC enhancement of p53 mutant KC clonal expansion is T-cell independent

Since LC may function as APC, we next assessed the contribution of $\alpha\beta$ and $\gamma\delta$ T cells to the mechanism of LC enhancement of p53 mutant KC clonal expansion. DTA mice were intercrossed to TCRβ–/– (deficient in all $\alpha\beta$ T cell populations) and TCRδ–/– (deficient in all $\gamma\delta$ T cell populations). LC-intact but T cell-deficient (TCRβ–/–δ–/–.NLC) mice were compared to LC-deficient and T cell deficient (TCRβ–/–δ–/–.DTA) mice for the development and expansion of p53 mutant KC islands under chronic UVB-exposure (Figure 4). In the complete absence $\alpha\beta$ or $\gamma\delta$ T cells, p53 island development and growth was again substantially enhanced in the presence of LC. Following 9 wks UVB exposure, p53 island density was 86% increased in TCRβ–/–δ–/–.NLC vs TCRβ–/–δ–/–.DTA (Figure 4a, 79.9 ± 4.5 vs $42.9 \pm 4.3/cm^2$, P<0.0001) and p53 island area was increased by 135% (Figure 4b, 10661 ± 1188 vs 4520 ± 711 μm^2 p53 island/mm^2, P=0.0004). The lack of requirement for $\alpha\beta$ T cells suggests that the mechanism does not involve LC stimulation of immunosuppressive $\alpha\beta$ Treg (Shreedhar *et al.*, 1998) or NKT cells (Fukunaga *et al.*, 2010) previously implicated in UV-induced immune suppression, $\gamma\delta$ T cells with the capacity for cytotoxicity of transformed KC (Girardi *et al.*, 2001), or pro-inflammatory $\alpha\beta$ (Kwong *et al.*, 2010) and $\gamma\delta$ (Wakita *et al.*, 2010) T cell subsets that might drive mutant KC proliferation. The striking parallel of the dependence on LC for increased p53 island number and size, as well as the LC association with the expanding p53 islands, observed in both T cell-intact (Figure 3d–i) and T cell-deficient (Figure 4c) mice, underscores the fundamental pro-tumor contribution of LC and suggested an underlying paracrine effect.

We thus sought to quantify within naïve and chronically UVB-irradiated TCRβ–/–δ–/–.NLC and TCRβ–/–δ–/–.DTA epidermis the expression levels of several epithelial growth factors previously implicated in paracrine stimulation of epithelial proliferation and neoplasia (Figure 4d): EGF (epidermal growth factor) (Chan *et al*., 2004), amphiregulin (AREG) (Rittié *et al*., 2006), insulin-like growth factor-1 (IGF-1) (DiGiovanni *et al*., 2000), keratinocyte growth factor-1/fibroblast growth factor-7 (KGF-1/FGF-7) (Jameson *et al*., 2002; Chikama *et al*., 2008), and IL-22 (Briso *et al*., 2012; Rabeony *et al*., 2014). Epidermal cells from non-irradiated skin of TCRβ–/–δ–/–.NLC and TCRβ–/–δ–/–.DTA revealed expression profiles consistent with constitutive expression of IL-22 within LC-intact epidermis (mean fold change untreated DTA = 1.0 ± 0.1 vs untreated NLC = 8.4 ± 2.1, P= 0.0023), with levels of such substantially elevated following chronic UVB exposure (DTA +UVB = 1.6 ± 0.1 vs untreated DTA, P = 0.0029; NLC+UVB = 52.5 ± 7.1 vs untreated NLC, P=0.0013,) and significantly higher in the presence of LC (DTA+UVB vs NLC+UVB, P<0.0001). In contrast, there were modest relative decreases or no discernible changes in the other assessed epithelial growth factors (Figure 4d). UVB-exposed LC-intact epidermis also displayed the highest levels of expression of IL-1β and IL-6, and to a lesser extent IL-23a (Figure 4e), cytokines known to stimulate production of IL-22 by adaptive αβ+ and γδ+ Th22 cells as well as innate immune cells, e.g. natural killer (NK) and innate lymphoid cells (ILC) (Ahlfors *et al*., 2014). Nitric oxide synthase 2, inducible (NOS2), known to foster reactive oxygen species within the epidermis after UVB exposure (Chang *et al*., 2003), was also highest in UVB-exposed LC-intact epidermis. Furthermore, exposure of purified LC to UVB *in vitro* resulted in increased expression of IL-1β, IL-6 and IL-23a (Supplemental Figure S6 online), suggesting that at least a portion of the observed epidermal expression of these cytokines was attributable directly to LC, as opposed to augmented production by KC in the presence of LC. Taken together, these data suggest that LC-intact epidermis demonstrates enhanced KC and/or LC production of IL-1β, IL-6, and (to a lesser extent) IL-23, which in turn supports local production of IL-22 by non-T (e.g. NK and/or ILC) cells.

IL-22 producing ILC3 populate chronically UVB-exposed skin

To determine the spectrum of immune cell populations present in T cell deficient LC-intact versus LC-deficient skin, suspensions prepared from TCRβ–/–δ–/–.NLC and TCRβ–/–δ–/ –.DTA mice were analyzed by flow cytometry (Supplementary Figure S7 online). The only discernible difference in CD45+ MHC-II+ cells from TCRβ–/–δ–/–.NLC relative to TCRβ –/–δ–/–.DTA skin was, as expected, the presence of LC populations (CD45+ MHCII+ CD11b+ CD207+ CD103−) that included epidermal LC as well as apparent dermal "in transit" migratory LC (Henri *et al.*, 2010). Although reduced in number following chronic UVB exposure, we found comparable levels between LC-intact and LC-deficient skin of the major dermal DC population (CD45+ MHCII+ CD11b+ CD207− CD103−), the minor Langerin+ dermal DC population (CD45+ MHCII+ CD11b− CD207+ CD103+), and other dermal (CD45+ MHCII+ CD11b− CD103−) DC. The epidermis of both TCRβ–/–δ–/–.NLC and TCRβ–/–δ–/–.DTA also harbors a population of CD45+ MHC-II− CD11b− IL-7R+ CD103+ cells that would be expected to contain innate lymphoid cells (ILC), and cells of this phenotype seemingly persist in UVB treated skin (Supplementary Figure S8 online). Isolation and further analysis of both protein (flow cytometry) and mRNA (qRT-PCR) expression (Figure 5) revealed the predominant differentiation phenotype to be consistent

with IL-22-producing RORγt+ (Tbet- GATA3-) group 3 innate lymphoid cells (ILC3) (rev. in Artis and Spits 2015). The proportion of CD45+ MHCII− epidermal ILC observed in TCRβ−/−δ−/− mice may be increased relative to that found in T cell intact mice, as a compensatory mechanism similar to that previously reported for various immune cell populations in genetically modified mouse models, including cutaneous ILC (Roediger *et al.*, 2013). Nonetheless, these ILC persist in chronically UVB exposed epidermis, unlike DETC, and expression of IL-22 by these cells was substantially higher in LC-intact epidermis after chronic UVB-exposure (Figure 5), consistent with their activation and differentiation being positively influenced by both the presence of LC and epidermal exposure to UVB.

The implication of LC herein as a major contributor to UVB-induced p53 mutant KC clonal expansion via the enhancement of local production of IL-22 by ILC3, independently of resident or infiltrating T cells, suggests that LC may also play a more general role in epidermal homeostasis, including supporting KC proliferation as part of the epidermal stress-response. Consistent with this hypothesis, at 5 weeks of UVB-exposure (a time with minimal difference in p53 island number and size between TCRβ−/−δ−/−.NLC and TCRβ−/−δ−/−.DTA; Figure 3d, e), we were able to detect greater epidermal thickness in association with the presence of LC (Figure 6a, b). Removal of the stratum corneum and superficial KCs by repetitive tapestripping (Kuo *et al.*, 2013) resulted in a greater transepidermal waterloss (TEWL) in TCRβ−/−δ−/−.NLC versus TCRβ−/−δ−/−.DTA epidermis (Figure 6c). More aggressive disruption of the epidermis by repetitive razor abrasion resulted in an even greater TEWL in LC-intact epidermis that showed histologic evidence of epidermal hyperplasia and hyperkeratosis (Figure 6d, e), and augmented expression of IL-22, IL-1β, and IL-23 (Supplementary Figure S9 online). Furthermore, a single application of TPA provoked a greater ear swelling response in LC-intact skin (Figure 6f), while chronic TPA application ultimately showed enhanced epidermal thickening in association with the presence of LC (Figure 6g). These data are all consistent with LC serving as fundamental contributors to the epidermal stress-response via stimulation of KC proliferation and dedifferentiation, independently of the presence of αβ and γδ T cells and regardless of the mode of epidermal damage (e.g. ultraviolet radiation, physical disruption, chemical irritant).

DISCUSSION

Immune cells resident within epithelial tissue play key roles in microbial defense and barrier homeostasis, and the activities of such cells may arrest or enhance carcinogenesis (Strid *et al.*, 2008; Yu *et al.*, 2014). The demonstration herein of a major role for LC in UVB induced skin carcinogenesis, as well as in the response to epidermal perturbation, further elucidates LC as fundamental regulators of epidermal homeostasis. The pro-carcinogenic effect of LC during UVB exposure is counter to the notion of LC as key players in tumor immunosurveillance. Moreover, the demonstration that the association of LC with p53 mutant KC clonal expansion is completely independent of the presence of αβ and γδ T cells favors a mechanism in which LC are directly affecting mutant KC and/or stimulating non-T (NK and/or ILC) immune cells to induce an intraepidermal environment conducive to mutant KC survival and growth.

During chronic UVB exposure, the LC network remained largely intact (Figure 3). Whether the observed LC numbers were reflective more of a relative resistance to apoptosis of the initial resident population of LC derived from fetal precursors, or from repopulating sources such as peripheral blood monocytes, is unclear. Nonetheless, Ki-67 staining reveals little evidence of active proliferation of LC, in contrast to the clonally expanding mutant KCs (Supplementary Figure S2 Online). The intimate association of LC with the clonally expanding KC islands suggests the possibility that LC detect and respond to dysregulated KC, or that the mutated KC produce chemoattractant and/or survival factors for the LC. Further investigation will be necessary to determine the relative contribution of LC enhancement to p53 mutant KC clonal expansion by direct (e.g. by local production of growth and/survival factors) versus indirect (e.g. by stimulation of other cells that produce growth and/or survival factors) influences, and whether the LC within expanding islands are functionally distinct from LC not found in association with mutant KC.

Our expression analysis of LC-intact and LC-deficient epidermal preparations, prior to and after chronic UVB exposure, has provided insight into the nature of LC promotion of clonal expansion. Epidermal relative expression of IL-1β, IL-6, and IL-23 were each observed to increase with UVB exposure in LC-deficient (TCRβ−/−δ−/−.DTA) skin, consistent with known production of these cytokines by stressed KCs. In the presence of LC (in TCRβ−/−δ−/−.NLC), UVB-induced expression was significantly enhanced for IL-1β and IL-6. Moreover, the substantial increase in expression of IL-1β in naïve LC-intact versus LC-deficient epidermis (i.e. prior to UVB exposure) suggest that LC may also be playing a role in homeostatic regulation of the epidermis. The augmented IL-22 expression observed in LC-intact skin chronically exposed to UVB is entirely consistent with increases in IL-1β, IL-6, and IL-23 – all known stimulators of IL-22 production.

Phenotypic analysis revealed that the augmented IL-22 production observed in association with the presence of LC and chronic UVB exposure may be attributable to RORγt+ ILC3 (rev. in Artis and Spits 2015). Thus, UVB-exposed LC-intact epidermis supports an environment for the augmented expression by ILC3 of IL-22, a cytokine noteworthy for its stimulation of KC proliferation and de-differentiation, skin wound healing, and well-established association with epithelial carcinogenesis (rev. in Lim and Savan, 2014). The receptor for IL-22 is primarily expressed by epithelial cells, including KC, as a heterodimer (IL-22R1 and IL-10R2) that stimulates Stat3 activation, and a pro-carcinogenic role for IL-22 has been shown in models of colonic, lung, and hepatocellular carcinoma. Moreover, IL-22-producing ILCs were shown to be the principal drivers of dysplasia in a model of inflammatory bowel disease-associated colorectal cancer (Kirchberger *et al.*, 2013).

The augmented local expression of IL-1β, IL-23, and IL-22 following razor abrasion in the presence of LC (Supplementary Figure S9 online) is also consistent with our observed responses to epidermal perturbation in (T cell-deficient) LC-intact skin: increased epidermal hypertrophy, compromised epidermal barrier function, and augmented irritant response (Figure 6). Recombinant IL-22 can promote the in vitro survival and proliferation of KCs after mechanical disruption (Eyerich et al., 2009) and epidermal hypertrophy and dedifferentiation in reconstituted human epidermis (Rabeony *et al.*, 2014). Since LC numbers are largely maintained in human AKs (Shevchuk *et al.*, 2014) and epidermal LC

levels in organ transplant recipients are equivalent to controls (Sandvik *et al.*, 2014), it is logical to investigate whether LC are contributing to human SCC development. Clearly, further studies are necessary to more fully elucidate the relationship of LC, ILC3, and IL-22 to epidermal homeostasis and UVB-induced cutaneous carcinogenesis.

MATERIALS AND METHODS

Animals and Housing

FVB/N LC-deficient hu-Langerin DTA transgenic (DTA), normal littermate controls (NLC), TCRβ–/–TCRδ–/– (TCRβ–/–δ–/–.NLC) and TCRβ–/–TCRδ–/–LC-deficient (TCRβ–/–δ–/–.DTA) mice were previously described (Modi *et al.*, 2012). Hairless mice (hr/hr, FVB/N background) were generously provided by Dr. Donna Kusewitt (The University of Texas MD Anderson Cancer Center, Houston, TX). All *in vivo* studies were approved by the Yale Animal Care and Use Committee.

UVB exposure

At age 7 wks, hair was removed from dorsal skin of female TCRβ–/–δ–/––.NLC and TCRβ–/–δ–/–.DTA mice by clipping plus depilatory cream; hr/hr mice were untreated. UVB exposures began at age 8 wks using a bank of four FS20T12 broadband-UVB bulbs (National Biological Corp.) with emitted light filtered (Kodacel TA422, Eastman Kodak Co.) to remove wavelengths <290nm. Exposure was monitored using a calibrated meter and probe (Intensity Meter 200, G&R Labs). Chronic exposure consisted of 400 J/m^2 3x/weekly.

Tumor assessment

Tumors were measured, counted (when   1 mm^2) and scored weekly as clinically apparent papillomas or carcinomas by a blinded observer as previously described (Girardi *et al.*, 2003). Tumor volume was calculated as: 4/3pi*r^3 where r = (LxW)/2.

Immunofluorescence and confocal microscopy

Epidermal sheets were prepared and stained as previously described (Lewis *et al.*, 2014) with anti-CD207 (RMUL.2, eBioscience), anti-TCRγδ (GL3, Becton Dickinson), anti-p53 (NCL-p53-CM5p, Leica Biosystems) followed by fluorescent species-specific secondaries (Jackson Immunoresearch). Z-stacked images (20/mouse) were collected (Zeiss 510Meta confocal) in a set pattern and Volocity 6.2 (Perkin Elmer, Waltham, MA) used to quantitate LC and DETC. CPD staining and quantification is described in Supplementary Figure S1 and p53 island quantification in Supplementary Figure S3.

Epidermal cell suspensions and flow cytometry

Epidermal cell suspensions were prepared as described (Strid *et al.*, 2008). For intracellular cytokine detection, cells were stimulated for 18 hr with 50 ng/ml PMA plus 1 μg/ml ionomycin. Monensin (2 μM) was added for the final 6 hr plus Brefeldin A (10 μg/ml) for the final 2 hr. Samples were blocked (2.4G2, BD Biosciences) and stained with antibodies to CD45 (30-F11, Biolegend), MHCII (M5/114.15.2, eBioscience), IL-22 (Poly5164, Biolegend) or isotype controls, plus viability dye EMA. BD Biosciences CytoFix/CytoPerm

kit was used for fixation and permeabilization. Data were collected on Stratedigm S1000EX and analyzed with FlowJo. Cell sorting, to obtain CD45+ MHCII− epidermal ILC, was performed on MoFlo (Beckman Coulter).

Gene expression analysis

RNA was isolated (RNeasy, Qiagen, Valencia, CA) and transcribed (High-Capacity cDNA Reverse Transcription kit, ABI, Carlsbad, CA). qRT-PCR (ABI 7500, SDS 2.0 software) was performed using Taqman assays and Taqman Gene Expression Mastermix (ABI). Ct values were normalized to β-actin and expression differences relative to untreated DTA calculated using RQ=$2^{-\Delta Ct}$.

Epidermal stress-response assays

TEWL was measured using the Tewameter TM300 (probe 06030433, Courage & Khazaka, Cologne, Germany). Tape-stripping consisted of 3 repetitions of adhesive tape application (Scotch Magic tape, 3M, St. Paul, MN) performed one week following hair removal. Epidermal abrasion was induced by twice repeated shaving of ventral skin (Personna American Safety Razor Co., Verona, VA). Ear thickness following a single application of TPA (Sigma, 0.5 nmoles) was measured using an engineer's micrometer (Mitutoyo 7301). Epidermal hypertrophy was induced by TPA (20 nmoles) application 2x/wk for 4 wks. Histologic examination and measurement of minimal epidermal thickness was performed as previously described (Lewis *et al.*, 2014),

Statistical analysis

Statistical significance of differences in tumor number and volume (Fig. 1) and ear thickness (Fig. 6f) over time were assessed using repeated measures ANOVA with Sidak's correction for multiple comparisons. Differences in relative gene expression were assessed using Student's t test for unpaired data with Holm-Sidak correction for multiple comparisons and establishment of significance. Other experimental groups were compared using one-tailed Student's t test for unpaired data with significance established at $P < 0.05$. All statistical analyses were performed with GraphPad Prism 6.0 software.

Supplementary Material

Refer to Web version on PubMed Central for supplementary material.

Acknowledgments

Abbreviations used in this paper

AK   actinic keratoses

CPD   cyclopyrimidine dimers

DC	dendritic cells
DETC	dendritic epidermal T cells
DMBA	dimethylbenz[a]anthracine
ILC	innate lymphoid cell
KC	keratinocyte
LC	Langerhans cells
DTA	LC-deficient hu-Langerin-DTA transgenic
NKT	natural killer T cell
NLC	normal littermate control
SCC	squamous cell carcinoma
TPA	12-O-tetradecanoylphorbol-13-acetate
UVB	ultraviolet B light

References

Aberer W, Romani N, Elbe A, et al. Effects of physicochemical agents on murine epidermal Langerhans cells and Thy-1-positive dendritic epidermal cells. J Immunol. 1986; 136:1210–6. [PubMed: 2868057]

Ahlfors H, Morrison PJ, Duarte JH, et al. IL-22 fate reporter reveals origin and control of IL-22 production in homeostasis and infection. J Immunol. 2014; 193:4602–13. [PubMed: 25261485]

Artis D, Spits H. The biology of innate lymphoid cells. Nature. 2015; 517:293–301. [PubMed: 25592534]

Bobr A, Igyarto BZ, Haley KM, et al. Autocrine/paracrine TGF-β1 inhibits Langerhans cell migration. Proc Natl Acad Sci U S A. 2012; 109:10492–7. [PubMed: 22689996]

Briso EM, Guinea-Viniegra J, Bakiri L, et al. Inflammation-mediated skin tumorigenesis induced by epidermal c-Fos. Genes Dev. 2013; 27:1959–73. [PubMed: 24029918]

Chan KS, Carbajal S, Kiguchi K, et al. Epidermal growth factor receptor-mediated activation of Stat3 during multistage skin carcinogenesis. Cancer Res. 2004; 64:2382–9. [PubMed: 15059889]

Chang HR, Tsao DA, Wang SR, et al. Expression of nitric oxide synthases in keratinocytes after UVB irradiation. Arch Dermatol Res. 2003; 295:293–6. [PubMed: 14615895]

Chikama T, Liu CY, Meij JT, et al. Excess FGF-7 in corneal epithelium causes corneal intraepithelial neoplasia in young mice and epithelium hyperplasia in adult mice. Am J Pathol. 2008; 172:638–49. [PubMed: 18276784]

Daya-Grosjean L, Robert C, Drougard C, et al. High mutation frequency in ras genes of skin tumors isolated from DNA repair deficient xeroderma pigmentosum patients. Cancer Res. 1993; 53:1625–9. [PubMed: 8453633]

DiGiovanni J, Bol DK, Wilker E, et al. Constitutive expression of insulin-like growth factor-1 in epidermal basal cells of transgenic mice leads to spontaneous tumor promotion. Cancer Res. 2000; 60:1561–70. [PubMed: 10749124]

Durinck S, Ho C, Wang NJ, et al. Temporal dissection of tumorigenesis in primary cancers. Cancer Discov. 2011; 1:137–43. [PubMed: 21984974]

Epstein JH. Photocarcinogenesis, skin cancer, and aging. J Am Acad Dermatol. 1983; 9:487–502. [PubMed: 6355213]

Eyerich S, Eyerich K, Pennino D, et al. Th22 cells represent a distinct human T cell subset involved in epidermal immunity and remodeling. J Clin Invest. 2009; 119:3573–3585. [PubMed: 19920355]

Fukunaga A, Khaskhely NM, Ma Y, et al. Langerhans cells serve as immunoregulatory cells by activating NKT cells. J Immunol. 2010; 185:4633–40. [PubMed: 20844203]

Girardi M, Oppenheim DE, Steele CR, et al. Regulation of cutaneous malignancy by gammadelta T cells. Science. 2001; 294:605–9. [PubMed: 11567106]

Girardi M, Glusac E, Filler RB, et al. The distinct contributions of murine T cell receptor (TCR)gammadelta+ and TCRalphabeta+ T cells to different stages of chemically induced skin cancer. J Exp Med. 2003; 198:747–55. [PubMed: 12953094]

Henri S, Poulin L, Tamoutounour S, et al. CD207+ CD103+ dermal dendritic cells cross-present keratinocyte-derived antigens irrespective of the presence of Langerhans cells. J Exp Med. 2010; 207:189–206. [PubMed: 20038600]

Ho KK, Halliday GM, Barnetson RS, et al. Topical and oral retinoids protect Langerhans' cells and epidermal Thy-1+ dendritic cells from being depleted by ultraviolet radiation. Immunology. 1991; 74:425–31. [PubMed: 1685145]

Jameson J, Ugarte K, Chen N, et al. A role for skin γδ T cells in wound repair. Science. 2002; 296:747–749. [PubMed: 11976459]

Kaplan DH, Jenison MC, Saeland S, et al. Epidermal langerhans cell-deficient mice develop enhanced contact hypersensitivity. Immunity. 2005; 23:611–20. [PubMed: 16356859]

Kirchberger S, Royston DJ, Boulard O, et al. Innate lymphoid cells sustain colon cancer through production of interleukin-22 in a mouse model. J Exp Med. 2013; 210:917–931. [PubMed: 23589566]

Kripke ML. Immunological unresponsiveness induced by ultraviolet radiation. Immunol Rev. 1984; 80:87–102. [PubMed: 6237978]

Kubo A, Nagao K, Yokouchi M, et al. External antigen uptake by Langerhans cells with reorganization of epidermal tight junction barriers. J Exp Med. 2009; 206:2937–46. [PubMed: 19995951]

Kuo IH, Carpenter-Mendini A, Yoshida T, et al. Activation of epidermal toll-like receptor 2 enhances tight junction function: implications for atopic dermatitis and skin barrier repair. J Invest Dermatol. 2013; 133:988–98. [PubMed: 23223142]

Kwong BY, Roberts SJ, Silberzahn T, et al. Molecular analysis of tumor-promoting CD8+ T cells in two-stage cutaneous chemical carcinogenesis. J Invest Dermatol. 2010; 130:1726–36. [PubMed: 19924136]

Lewis JM, Bürgler CD, Fraser JA, et al. Mechanisms of Chemical Cooperative Carcinogenesis by Epidermal Langerhans Cells. J Invest Dermatol. 201410.1038/jid.2014.411

Lim C, Savan R. The role of the IL-22/IL-22R1 axis in cancer. Cytokine Growth Factor Rev. 2014; 25:257–71. [PubMed: 24856143]

MacLeod AS, Rudolph R, Corriden R, et al. Skin-resident T cells sense ultraviolet radiation-induced injury and contribute to DNA repair. J Immunol. 2014; 192:5695–702. [PubMed: 24808367]

Merad M, Manz MG, Karsunky H, et al. Langerhans cells renew in the skin throughout life under steady-state conditions. Nat Immunol. 2002; 3:1135–41. [PubMed: 12415265]

Modi BG, Neustadter J, Binda E, et al. Langerhans cells facilitate epithelial DNA damage and squamous cell carcinoma. Science. 2012; 335:104–8. [PubMed: 22223807]

Nishibu A, Ward BR, Jester JV, et al. Behavioral responses of epidermal Langerhans cells in situ to local pathological stimuli. J Invest Dermatol. 2006; 126:787–96. [PubMed: 16439974]

Rabeony H, Petit-Paris I, Garnier J, et al. Inhibition of keratinocyte differentiation by the synergistic effect of IL-17A, IL-22, IL-1a, TNFa and oncostatin M. PLoS One. 2014; 9(7):e101937. [PubMed: 25010647]

Rittié L, Varani J, Kang S, et al. Retinoid-induced epidermal hyperplasia is mediated by epidermal growth factor receptor activation via specific induction of its ligands heparin-binding EGF and amphiregulin in human skin in vivo. J Invest Dermatol. 2006; 126:732–9. [PubMed: 16470170]

Roediger B, Kyle R, Yip K, et al. Cutaneous immunosurveillance and regulation of inflammation by group 2 innate lymphoid cells. Nat Immunol. 2013; 14:564–573. [PubMed: 23603794]

Sandvik LF, Skarstein K, Sviland L, et al. CD11c(+) dendritic cells rather than Langerhans cells are reduced in normal skin of immunosuppressed renal transplant recipients. Acta Derm Venereol. 2014; 4:173–8. [PubMed: 23995623]

Seneschal J, Clark RA, Gehad A, et al. Human epidermal Langerhans cells maintain immune homeostasis in skin by activating skin resident regulatory T cells. Immunity. 2012; 36:873–84. [PubMed: 22560445]

Seré K, Baek JH, Ober-Blöbaum J, et al. Two distinct types of Langerhans cells populate the skin during steady state and inflammation. Immunity. 2012; 37:905–16. [PubMed: 23159228]

Shreedhar VK, Pride MW, Sun Y, et al. Origin and characteristics of ultraviolet-B radiation-induced suppressor T lymphocytes. J Immunol. 1998; 161:1327–35. [PubMed: 9686595]

Shevchuk Z, Filip A, Shevchuk V, et al. Number of Langerhans cells is decreased in premalignant keratosis and skin cancers. Exp Oncol. 2014; 36(1):34–7. [PubMed: 24691282]

Strid J, Roberts SJ, Filler RB, et al. Acute upregulation of an NKG2D ligand promotes rapid reorganization of a local immune compartment with pleiotropic effects on carcinogenesis. Nat Immunol. 2008; 9:146–54. [PubMed: 18176566]

Wakita D, Sumida K, Iwakura Y, et al. Tumor-infiltrating IL-17-producing gammadelta T cells support the progression of tumor by promoting angiogenesis. Eur J Immunol. 2010; 40:1927–37. [PubMed: 20397212]

Wang L, Jameson SC, Hogquist KA. Epidermal Langerhans cells are not required for UV-induced immunosuppression. J Immunol. 2009; 183:5548–53. [PubMed: 19843938]

Yu SH, Bordeaux JS, Baron ED. The immune system and skin cancer. Adv Exp Med Biol. 2014; 810:182–91. [PubMed: 25207366]

Zhang W, Remenyik E, Zelterman D, et al. Escaping the stem cell compartment: sustained UVB exposure allows p53-mutant keratinocytes to colonize adjacent epidermal proliferating units without incurring additional mutations. Proc Natl Acad Sci U S A. 2001; 98:13948–53. [PubMed: 11707578]

Ziegler A, Jonason AS, Leffell DJ, et al. Sunburn and p53 in the onset of skin cancer. Nature. 1994; 372:773–6. [PubMed: 7997263]
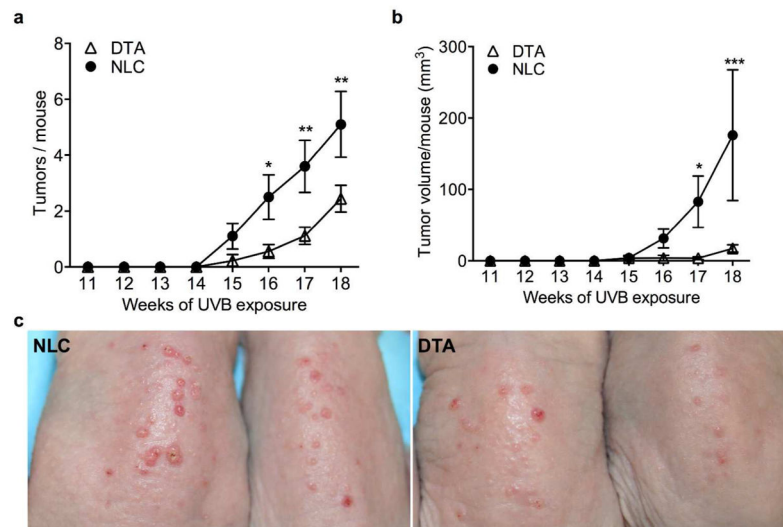
Figure 1. Langerhans cells influence UVB-induced cutaneous tumor development
Carcinogenesis was induced in hairless (hr/hr) LC-intact (NLC) and LC-deficient (DTA) mice by exposure to 400 J/m^2 UVB three times per week. Increased tumor number **(a)** and volume **(b)** were seen in the presence of LC (n=10 NLC, 9 DTA, * P<0.05, **P<0.01, ***P<0.001). (**c**) Representative images from (a, b).
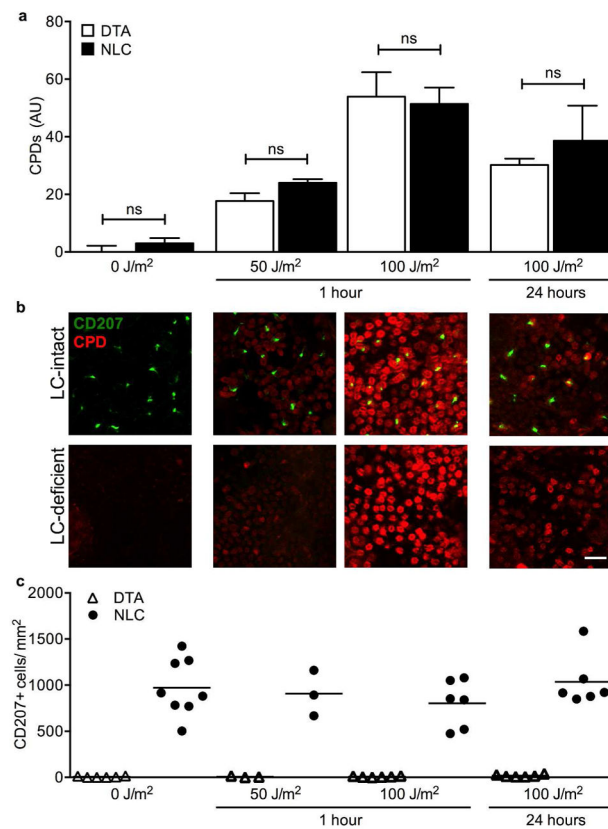
Figure 2. Langerhans cells do not affect UVB-induced CPD formation
(**a**) Hairless (hr/hr) LC-intact (NLC) and LC-deficient (DTA) mice were treated with a single dose of UVB and epidermal sheets prepared 1 or 24 hr later and stained with antibodies directed against thymine dimers (CPD) and CD207 plus the nuclear dye To-Pro-3 (shown in Supplementary Figure S1 online). CPD fluorescence intensity was similar in LC-intact and LC-deficient mice. (**b**) Representative images from (a) show CPD (red) and LC (CD207, green). Scale bar = 20 μm. (**c**) LC density does not change during the 24 hrs following a single dose of UVB. n=3–8 mice/group; in (c) each symbol represents one mouse.
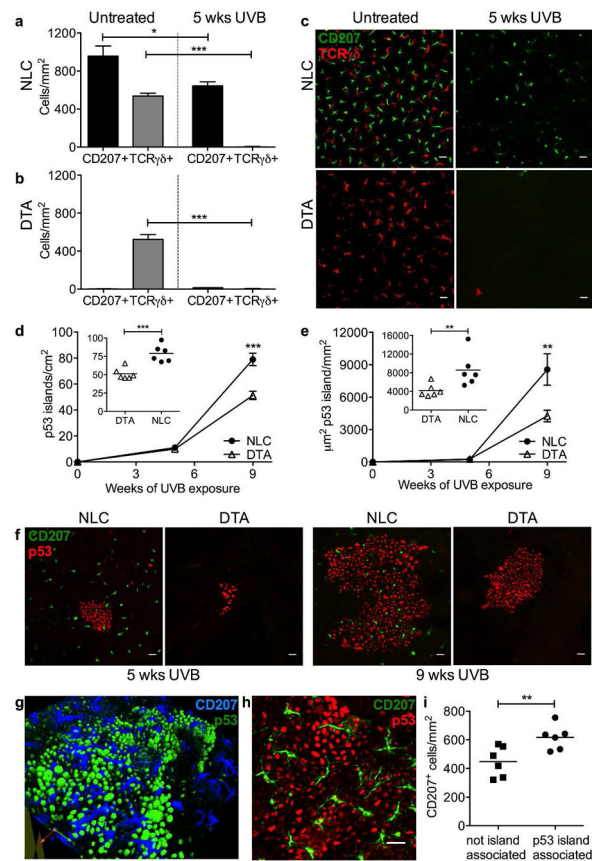
Figure 3. Langerhans cells persist during chronic UVB exposure and facilitate p53 island formation

CD207+ LC and TCRγδ+ DETC were quantified in epidermal sheets prepared from untreated vs chronic UVB treated (400 J/m², 3x/wk, 5 wks) LC-intact NLC (**a**) and LC-deficient DTA (**b**) hr/hr mice. Representative images (**c**) show CD207 (green) and TCRγδ (red) staining. In both NLC and DTA mice, DETC are nearly eliminated by chronic UVB treatment, however LC in NLC mice are present at 66% of control levels following 5 wks UVB; *P<0.5, ***P<0.001, n=6 mice/group. Mutant KC p53 island density (**d**) and area (**e**) were quantified in epidermal sheets prepared from n=6 NLC and DTA hr/hr mice following 5 or 9 wks UVB exposure. Inset graphs show distribution at 9 wks; each symbol represents one mouse, **P<0.01, ***P<0.001. Representative images (**f, h**) of p53 islands (red) and CD207+ LC (green), scale bar = 20 μm, and a 3D rendering (**g**) of p53 (green) and LC (blue). CD207+ LC density (**i**) is increased in association with p53 islands; **P<0.01. Quantitation is described in Supplementary Figure S3 online.
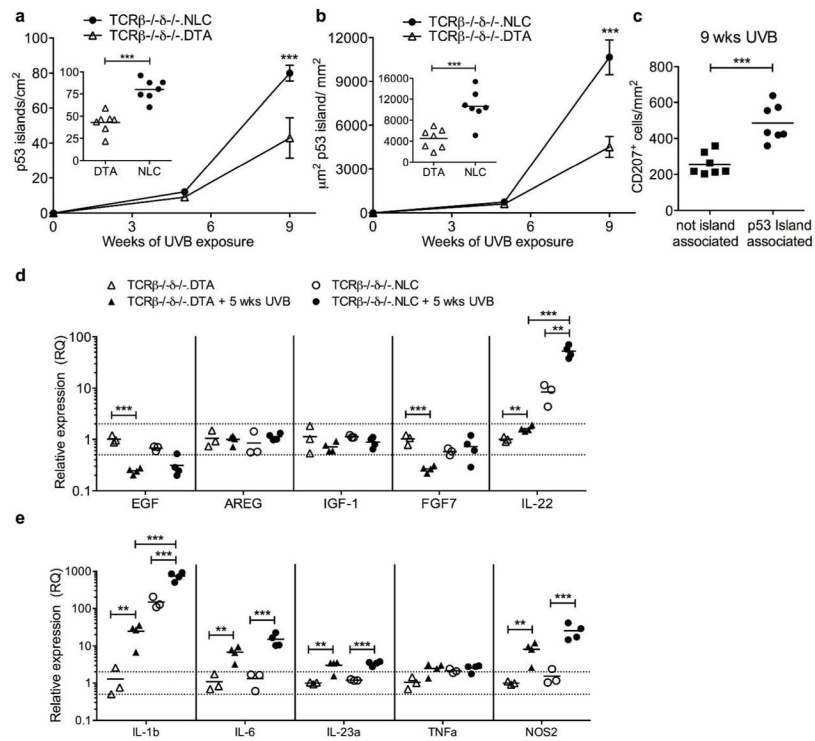
Figure 4. LC facilitation of p53 island growth is T cell independent

Mutant KC p53 island density (**a**) and area (**b**) were quantified in epidermal sheets prepared from TCRβ−/−δ−/−.NLC and TCRβ−/−δ−/−.DTA mice following 5 or 9 wks UVB exposure (400 J/m^2, 3x/wk). Inset graphs show distribution at 9 wks; each symbol represents one mouse. LC-intact TCRβ−/−δ−/−.NLC mice have increased p53 island density and area compared to LC-deficient TCRβ−/−δ−/−.DTA mice following 9wks UVB; ***P<0.001. (**c**) CD207+ LC density is increased in association with p53 islands. (**d, e**) Epidermal cells prepared from untreated vs 5 wk chronic UVB treated TCRβ−/−δ−/−.NLC and TCRβ−/−δ−/−.DTA mice were examined for changes in gene expression (relative to untreated TCRβ−/−δ−/−.DTA) by qRT-PCR; each symbol represents one mouse,**P<0.01, ***P<0.001, Holm-Sidak correction for multiple comparisons.
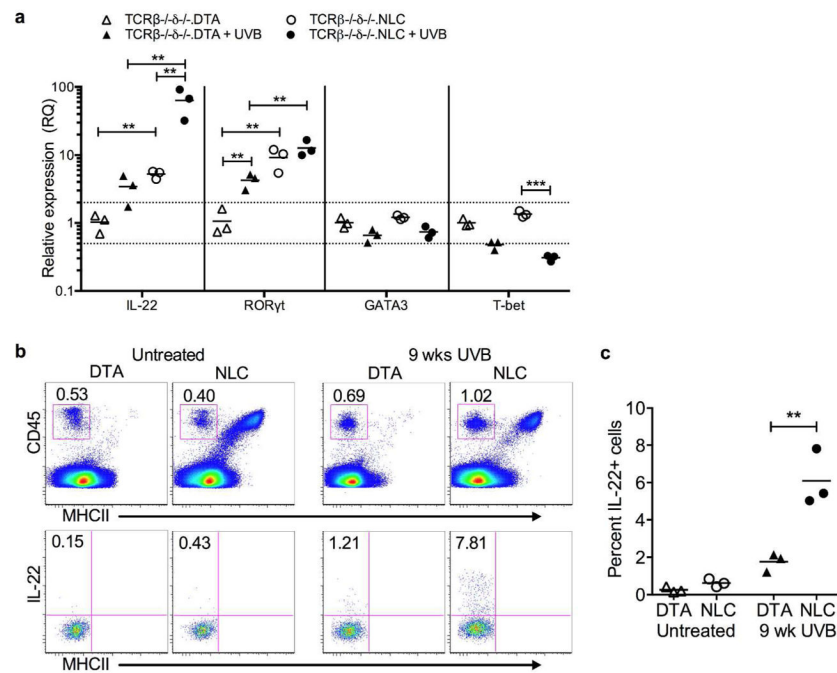
Figure 5. Epidermal innate lymphoid cells (ILC) produce IL-22 in response to chronic UVB exposure in the presence of LC

(**a**) Epidermal ILC were purified from untreated and chronic UVB treated (9 wks, 400 J/m^2, 3x/wk) TCRβ−/−δ−/−.NLC and TCRβ−/−δ−/−.DTA mice by flow cytometric sorting and changes in gene expression (relative to untreated TCRβ−/−δ−/−.DTA) assessed by qRT-PCR; each symbol represents one mouse, **P<0.01, ***P<0.001, Holm-Sidak correction for multiple comparisons. (**b**) Epidermal cells from individual untreated and 9 wk chronic UVB treated TCRβ−/−δ−/−.NLC and TCRβ−/−δ−/−.DTA mice were stimulated with PMA + Ionomycin IL-22 production assessed by flow cytometry. Top panels show CD45+ MHCII− gating, lower panels are gated on CD45+ MHCII− cells. Plots are representative of n=3 mice/group. (**c**) Percentage of IL-22 producing CD45+ MHCII− epidermal cells; each symbol represents one mouse, **P<0.01.
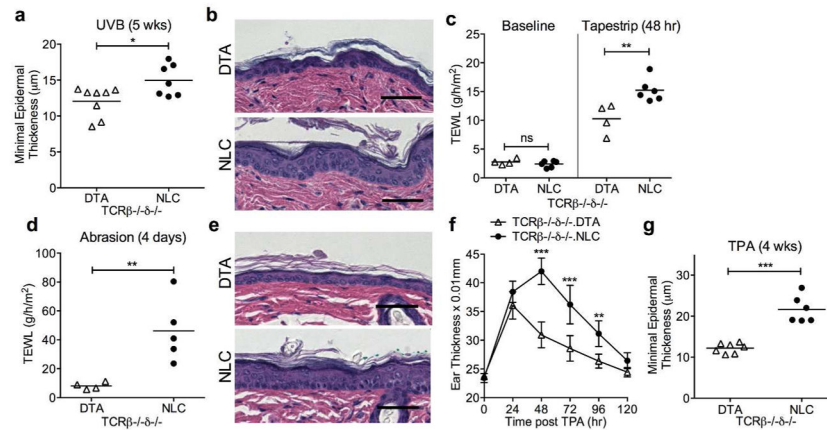
Figure 6. LC contribute to the epidermal stress response in a T cell independent manner
(**a**) Epidermal hypertrophy is greater in LC-intact TCRβ–/−δ–/−.NLC than in LC-deficient
TCRβ–/−δ–/−.DTA mice following chronic UVB exposure (400 J/m^2, 3x/wk, 5wks) as
evaluated by measuring the minimal epidermal thickness. (**b**) Representative images of (a).
Transepidermal waterloss (TEWL) is equivalent at baseline, but increased in LC-intact mice
48hr after tapestripping (**c**) as well as 4 days after epidermal abrasion by repetitive razor
shaving (**d**). (**e**) Representative images of (d). Ear thickness following a single TPA
application (**f**) and minimal epidermal thickness following twice weekly TPA for 4 wks (**g**)
are greater in the presence of LC. Each symbol represents one mouse in panels a, c, d and f;
n=7 NLC and 7 DTA in panel g.